CHEMISTRY & SUSTAINABILITY

CHEMSUSCHEM

ENERGY & MATERIALS

Accepted Article

Title: Investigation of methane oxidation reactions over Lanthanum Manganites-Pd/YSZ dual bed by 18O labeling-DRIFTS coupling

Authors: Melissandre Richard, Daniel Duprez, Nicolas Bion, and Fabien Can

This manuscript has been accepted after peer review and appears as an Accepted Article online prior to editing, proofing, and formal publication of the final Version of Record (VoR). This work is currently citable by using the Digital Object Identifier (DOI) given below. The VoR will be published online in Early View as soon as possible and may be different to this Accepted Article as a result of editing. Readers should obtain the VoR from the journal website shown below when it is published to ensure accuracy of information. The authors are responsible for the content of this Accepted Article.

To be cited as: *ChemSusChem* 10.1002/cssc.201601165

Link to VoR: http://dx.doi.org/10.1002/cssc.201601165

A Journal of ChemPubSoc Europe

WILEY-VCH

www.chemsuschem.org

Investigation of methane oxidation reactions over Lanthanum Manganites-Pd/YSZ dual bed by ^{18}O labeling-DRIFTS coupling

Melissandre Richard,[a] Daniel Duprez,[a] Nicolas Bion[a] and Fabien Can,*,[a]

Abstract: Low loading palladium supported yttrium-stabilized zirconia ($0.2\%_{wt}$Pd/YSZ) and $LaMnO_3$ perovskite were associated to study the partial oxidation of methane using labeled $^{18}O_2$ in the gas phase. Synthesis gas production was demonstrated to occur via an indirect reaction where oxygen is first consumed in the total methane combustion. A Mars-Van-Krevelen mechanism was observed over Pd/YSZ at 425°C to yield $C^{16}O_2$ and $C^{16}O$. A significant enhancement of the Pd/YSZ catalyst activity was achieved by the association of $LaMnO_3$+Pd/YSZ in a dual catalyst bed. It results a significant increase of the oxidation rate. Vibration bands of adsorbed formate species, assumed as intermediate to synthesis gas production, were observed by DRIFTS coupling experiments. It was proposed that $LaMnO_3$ enables the generation of highly active singlet O_2 which is activated on the YSZ oxygen vacancies to assist a rapid recovery of surface PdO and increase formate decomposition into CO and H_2 in Pd-supported catalyst.

Introduction

Methane is the main component of natural gas. It is also present in great proportion in biogas and shale gas. The proven reserves of natural gas would be close to $2x10^{14}$ m^3 in 2013 while the production of biogas amounts to 10^{12} m^3/year in Europe.[1] Methane combustion (Eq. 1) is widely used in industry to produce heat and electricity.

$$CH_4 + 2O_2 \rightarrow CO_2 + 2H_2O \qquad \Delta H^{0}_{298} = -\mathbf{802\ kJ\ mol^{-1}} \qquad (1)$$

The reaction can be catalyzed by noble metals [2,3] or oxides such as perovskites.[4] The main problem in combustion processes is to control the temperature of reaction to avoid NOx formation when air, instead of oxygen, is used as combustion agent. But methane is also a feared greenhouse gas whose global warming potential (GWP) is 25 times that of carbon dioxide at a time horizon of 100 years [5] even though a GWP of 10 has been reported in the past.[6] As CH_4 is mixed in flue gases with more reactive compounds, it is essential to improve the catalyst activity to get CH_4 oxidation at the lowest possible temperature.

Partial oxidation (Eq. 2) is an alternative process to transform methane into synthesis gas, a more valuable product than those of total oxidation with a suitable H_2/CO ratio of 2 for downstream processes such as methanol synthesis and Fischer-Tropsch synthesis for instance.[7,8]

$$CH_4 + \tfrac{1}{2}O_2 \rightarrow CO + 2H_2 \qquad \Delta H^{0}_{298} = -\mathbf{35.7\ kJ\ mol^{-1}} \qquad (2)$$

As for total oxidation, noble metals [9] or perovskites [4] can be used for producing synthesis gas with excellent yield. Depending on the CH_4:O_2 ratio, methane conversion can be selectively oriented, on the same catalyst, towards Eq. 1 or 2, but not necessarily at the same temperature. It is reported that partial oxidation of methane (POM) may occur via two different mechanisms, *i.e.*, direct POM, assuming that methane is directly converted to CO and H_2 without initial deep oxidation, or indirect POM. In this latter case, oxygen is claimed to be first consumed in the combustion reaction (Eq. 1). The remaining methane is converted to synthesis gas by dry or steam reforming.

The relevance of using Lanthanum Manganites-Pd/YSZ dual catalytic bed for methane oxidation at moderate temperature was explained in our recent works.[10,11] Remarkable performances were obtained on yttrium-stabilized zirconia-based palladium (0.2 wt-% Pd / $8\%_{mol}Y_2O_3$-ZrO_2 noted Pd/YSZ) in both $^{18}O_2$/$^{16}O_2$ exchange activity and methane oxidation when $LaMnO_3$ perovskite was placed in a first bed upstream. These results were suggested to be related to the formation of highly active singlet oxygen species through $LaMnO_3$ bed facilitating the activation of O_2 molecule on the YSZ surface from 425°C. The concentration of oxygen vacancies in the YSZ oxide played also an important role in oxygen activation. The latter allowed a drastic improvement of methane oxidation rate in dual-bed system inducing the participation of oxygen atoms of YSZ solid through a *Mars-van Krevelen (MvK)* mechanism.

The purpose of the present study was to investigate the partial oxidation of methane over the same dual-bed system by coupling *in situ* infrared spectroscopy and mass spectrometry (MS) analysis. A DRIFTS (diffuse reflectance infrared Fourier transform spectroscopy) cell was added to isotopic exchange set-up enabling both gas phase and surface study to highlight adsorbed intermediate species in dual-bed configuration.

Results and Discussion

Catalytic systems for methane oxidation

^{18}O labeling-DRIFTS coupling was used to study the four following catalytic systems for partial methane oxidation (POM) reaction, namely $LaMnO_3$ single solid (denoted hereafter as LM), Pd/YSZ, LM-YSZ and LM-Pd/YSZ dual-beds. Note that the ratio $40\%_w$ LM and $60\%_w$ YSZ or Pd/YSZ was chosen for dual-bed composition according to previous results.[11] The reaction was performed at

---

[a] Dr. M. Richard, Dr. D. Duprez, Dr. N. Bion, Dr. F. Can
University of Poitiers, CNRS, UMR 7285
Institut de Chimie des Milieux et Matériaux de Poitiers (IC2MP)
4 rue Michel Brunet – TSA 51106 – 86073 Cedex 9, France
E-mail: fabien.can@univ-poitiers.fr

Supporting information for this article is given via a link at the end of the document.

Accepted Manuscript

This article is protected by copyright. All rights reserved.

425°C with CH_4:$^{18}O_2$ (2:1 molar ratio) reactive mixture in the closed recycling device (see experimental section).

Figure 1 compares the four catalytic formulations on the basis of $^{18}O_2$ (*m/z* 36) conversion and H_2 (*m/z* 2) production versus time on stream. Note that single YSZ solid does not exhibit any activity at 425°C, in agreement with previous work that showed a high temperature activity of yttrium-stabilized zirconia for methane oxidation.[12]

As previously reported [10], two steps are identified according to the evolution of the reaction products: (a) in the first minutes of reaction, a rapid consumption of CH_4 and $^{18}O_2$ is observed simultaneously with an increasing of CO_2 (Figure 2B) and H_2O signals (*see supporting information, Figure S1*). Clearly, only methane combustion reaction occurs in this step; (b) then, after the almost total consumption of O_2, the partial methane oxidation could explain the concomitant appearance of syngas H_2 and CO. The main advantage of this reaction procedure is to have an overview of the performance of the catalytic system both in methane combustion and in partial oxidation (POM).

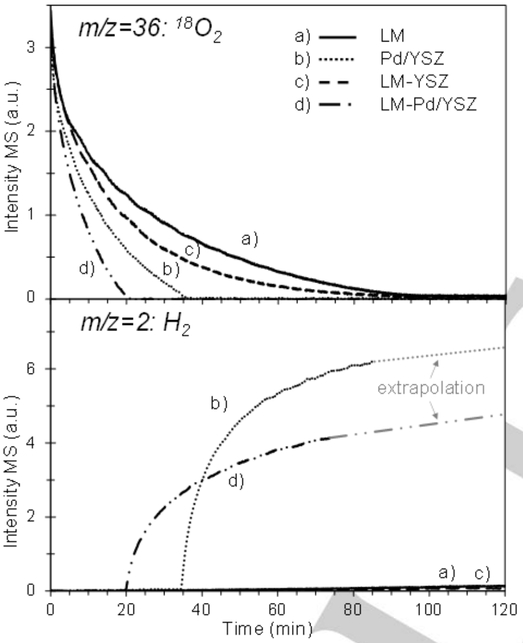

Figure 1. Time evolution of m/z=2 and 36 (H_2 and $^{18}O_2$) signals during POM reaction at 425°C over a) LM, b) Pd/YSZ single beds and c) LM-YSZ, d) LM-Pd/YSZ dual-beds.

Differences in catalytic activity occur for both steps over the four catalytic systems. First, combustion of methane is enhanced when LM is placed upstream compared to corresponding single YSZ or Pd/YSZ beds. In a very recent work, it was demonstrated by oxygen isotopic exchange that $LaMnO_3$ activates the O_2 molecule on the YSZ oxygen vacancy sites resulting in significant improvement in total methane oxidation activity.[10,11] Then, H_2 production was observed only for supported-Pd catalysts (curves b) and d)). As expected, the presence of Pd (or PdO) particles is crucial at this temperature to produce H_2 in the second reaction step. Even if the nature of active sites of Pd-based catalysts for methane oxidation has been a matter of debate, Farrauto *et al*.[13] conclude that activity of a supported-palladium catalyst is due to the ability of palladium oxide (PdO_x) to chemisorb oxygen. Additionally, Takahashi *et al*.[14] agree that PdO enhances oxygen adsorption, lowering the activation energy for methane oxidation. The methane combustion step is then assumed to result in a PdO/Pd redox combustion mechanism serving as porthole for gas phase oxygen to dissociate, migrate to the oxide support, and exchange with oxygen from the oxide support. Additionally, mechanisms for the combustion of methane over PdO-based catalysts need to include steps for oxygen and hydroxyl exchange between the Pd phase and the support.[15] The best catalytic performances were obtained on dual LM-Pd/YSZ bed for which the production of H_2 occurs after only 20 min compared to 35 min for Pd/YSZ. This result highlights the beneficial impact of the $LaMnO_3$ placed upstream on both methane combustion and POM reaction.

Furthermore, products containing ^{16}O atoms from bulk YSZ catalyst are first observed in gas phase during both steps of reaction ($C^{16}O_2$, then $C^{16}O$). It is thus confirmed that the reaction proceeds through a *Mars-van Krevelen* (*MvK*) mechanism, in which methane is oxidized by lattice oxygen ions on the surfaces of YSZ. To the opposite, for LM perovskite tested alone, labelled $C^{18}O_2$ is first observed during methane combustion, illustrating *suprafacial* mechanism where lattice oxygen of this solid are not involved in the reaction in our conditions.

^{18}O labeling-DRIFTS coupling on Pd/YSZ catalyst

IR bands corresponding to the formation of gaseous CH_4 and CO_2 species were observed during POM reaction over LM-Pd/YSZ system (*see supporting information, Figure S2*). But in this case the adsorbed species were not detected on perovskite surface due to a low IR reflection of the black material. Therefore ^{18}O labelling-DRIFTS coupling was focused on Pd/YSZ single bed, since essential steps of the CH_4 reaction are located on this catalyst. Figure 2A shows the DRIFTS spectra recorded during methane oxidation reaction on Pd/YSZ catalyst at 425°C in which typical IR bands corresponding of gaseous CH_4 (at 3015 and 1304 cm^{-1}) and CO_2 (broad bands at 2260-2400 cm^{-1}) were also observed. After 35 min of reaction, new IR bands appeared in the range of 1675-2095 cm^{-1} which can be attributed to the formation of carbon monoxide adsorbed on Pd. A detailed assignment of these IR bands is given in the next section. Moreover, the discrete appearance of 2143 cm^{-1} centered IR band after 40 min of reaction seems to confirm the $C^{16}O$ formation in gas phase. Note also the occurrence of two negative bands at 3684 and 3640 cm^{-1} in the OH region. This hydroxyl groups can probably participate in the formation of intermediate adsorbed species such as hydrogen-carbonate ($HCO_3^–$), formate ($HCOO^–$) or acetate ($CH_3COO^–$) species.

The variations with time of IR bands areas are plotted in Figure 2B for $CH_{4(g)}$, $CO_{2(g)}$ and $CO_{(ads)}$ and compared to MS profiles. A correlation can clearly be observed between DRIFTS and MS data. At the beginning of the experiment (<35 min), the rapid rise of the CO_2 concomitant with the decrease of CH_4 bands integration observed by infrared spectroscopy confirms that methane combustion is the predominant pathway. During this first step, sufficient oxygen concentration allows the total oxidation of

Accepted Manuscript

This article is protected by copyright. All rights reserved.

10.1002/cssc.201601165

surface species to CO_2 and H_2O. The IR bands of adsorbed carbonyl species quickly emerged after 35 min of reaction to reach a maximum at 40 min before their slowly decay. At the same time, MS profile showed the formation of H_2 (*m/z* 2) and $C^{16}O$ (*m/z* 28) in gaseous phase. Water-gas shift (WGS) reaction between CO and H_2O and methane decomposition cannot be excluded to explain, in part, the observed H_2 production. The possible occurrence of WGS could also justify the small increase of $CO_{2(g)}$ during the second step of reaction. In contrast, the fact that CO_2 was not consumed when H_2 and CO are emitted indicates that partial oxidation of methane to synthesis gas did not involve dry reforming reaction at 425°C. We previously propose two reactions to explain the hydrogen formation, namely steam reforming and direct partial oxidation of CH_4 with lattice oxygen atoms. The evolution of the curve corresponding to 18 m/z (*see supporting information, Figure S1*) does not allow validating the former reaction at 425°C, whereas the latter reaction has been observed when CH_4 was introduced alone at the same temperature on the dual-bed reactor, in agreement with the results of Lefferts *et al*.[12]

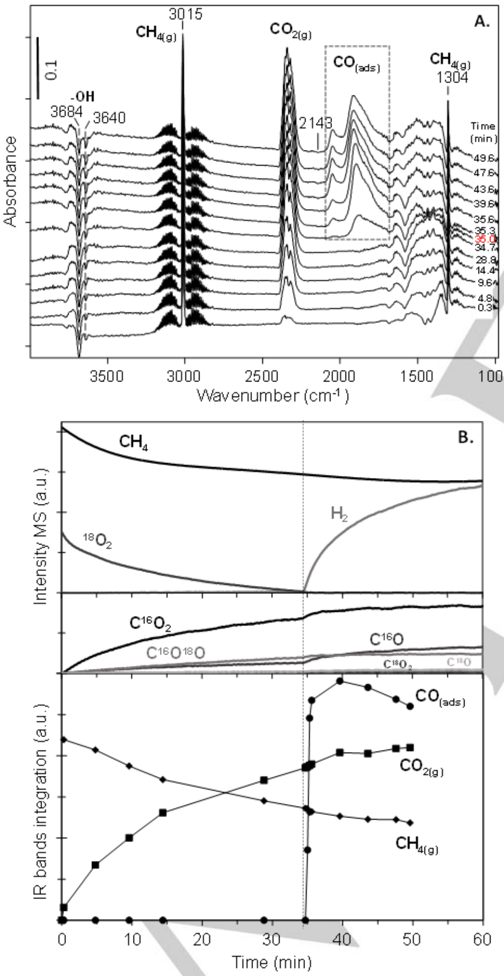

Figure 2. POM reaction over Pd/YSZ at 425°C. **A.** DRIFTS spectra vs. time. **B.** Comparison between MS profiles and IR band integrations.

In addition, the rise from 425°C to 700°C (rate 10°C/min) after 90 min of POM reaction leads to the desorption of adsorbed carbonyl species from catalyst surface together with a decrease of $CH_{4(g)}$ and $CO_{2(g)}$ IR bands (*see supporting information, Figure S3*). To the contrary, centered bands at 2143 and 2093 cm^{-1} are clearly distinguished and assigned to $C^{16}O$ and $C^{18}O$ gaseous molecules respectively.

To confirm the formation of carbon monoxide in the second step of reaction and the assignment of IR bands observed in the range of 1675-2093 cm^{-1}, the same POM experiment was performed at 425°C on a pre-exchanged Pd-YSZ catalyst, *i.e.* after introduction of a significant amount of $^{18}O_{(s)}$ in YSZ lattice (see experimental section). The observed MS profiles of $C^{16}O$ (*m/z* 28) and $C^{18}O$ (*m/z* 30) are represented in Figure 3A. As expected with this pre-exchanged material, the formation of labeled molecule was mainly detected in the gas phase. Figure 3B shows a comparison of DRIFTS spectra for (a) raw and (b) pre-exchanged Pd-YSZ bed in the range of 1700-2400 cm^{-1}. An isotopic shift of 47 and 37 cm^{-1} to lower wavenumber was clearly observed for IR bands at 2056 and 1915 cm^{-1} respectively. Note that the shift was also significant concerning $CO_{2(g)}$ bands. An uniform isotopic shift, corresponding to a frequency ratio (i = $\nu C^{16}O/\nu C^{18}O$) of 1.02 between corresponding wavenumbers of spectra (a) and (b), demonstrates their assignments to the same carbonyl species adsorbed on Pd.

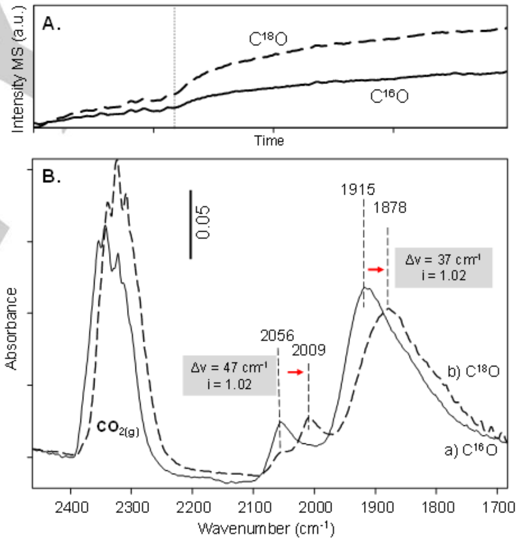

Figure 3. A. MS signals of $C^{16}O$ and $C^{18}O$ (*m/z* 28 and *m/z* 30) recorded during POM reaction at 425°C over $^{18}O_2$ pre-exchanged Pd/YSZ catalyst. **B.** Comparison of DRIFTS spectra between (a) raw and (b) pre-exchanged Pd/YSZ materials with $^{18}O_2$.

CO adsorption experiments

The assignment of adsorbed carbonyl bands observed on Pd/YSZ surface by ^{18}O labeling-DRIFTS coupling was studied in more details by performing CO adsorption experiments. Stretching vibration frequencies of the adsorbed molecules were measured in different steady-state conditions, described below, and compared to the literature and POM experimental results (Figure 4). The first experiment was carried out in a closed FTIR cell containing a self-supporting wafer of Pd/YSZ material (c.a. 15

Accepted Manuscript

This article is protected by copyright. All rights reserved.

mg.cm^{-2}). Successive doses of carbon monoxide (Pressure = 0.1 to 100 mbar in a volume of 0.9 cm^3) were introduced at ambient temperature on the wafer pre-reduced in H_2 at 450 °C and then evacuated at 10^{-6} mbar. Spectrum (a) was recorded after saturation of the surface by CO pulses. Two other experiments were carried out in the DRIFTS cell containing 100 mg of catalyst. After the same oxidative pre-treatment at 700°C than the one used prior to the POM reaction, 30 mbar of CO was admitted in the cell at 425°C. Spectra (b) and (c) were recorded at 425°C and after cooling down to room temperature respectively.

Figure 4 presents these normalised IR spectra in the range of 1700-2200 cm^{-1}, compared with that recorded during POM reaction at 425°C (spectrum d)). Note that the presence of gaseous molecule was observed with centered IR band at 2143 cm^{-1}. Metallic palladium forms carbonyls that are generally characterized by bands at wavenumbers below 2100 cm^{-1}, due to the back-donation of electrons from the metal d bands to CO $2\pi^*$ antibonding orbital. Additionally, the vibrational frequencies of the C−O bond stretching depend on the different adsorption sites of CO on Pd.[16] Generally, the ν(CO) bound around 2100 cm^{-1} is assigned to linearly bound CO molecules.[17] CO adsorbed on bridge sites presents distinct features in IR spectra below 2000 cm^{-1}. To the opposite, the spectral ranges in which IR bands have been attributed to surface carbonyls of Pd^{n+} are ranked between 2215-1930 cm^{-1}. Linear Pd^{2+}−CO complexes were observed at 2215-2145 cm^{-1}; Pd^+−CO species are characterized by bands between 2140 and 2110 cm^{-1} and bridging carbonyls Pd^+−CO−Pd^+ were suggested to absorb in the range 1995-1975 cm^{-1}.[16]

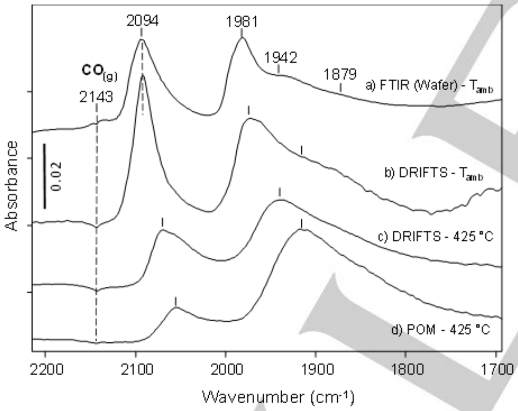

Figure 4. CO adsorption spectra over Pd/YSZ. Experimental conditions: (a) Transmission FTIR cell at ambient temperature; DRIFTS cell (b) at ambient temperature, (c) at 425°C and (d) during POM reaction at 425°C.

Spectrum (a) shows four stretching bands of carbonyl species (νCO) adsorbed on Pd/YSZ surface at 2094, 1981, 1942 (shoulder) and 1879 (shoulder) cm^{-1}. These bands were assigned to different Pd adsorption sites, listed in Table 1, in accordance with previous studies on oxide supported-Pd systems [18,19]. IR vibration bands observed on spectra recorded in the DRIFTS cell were attributed by analogy with the bands listed in Table 1. Additionally, adsorbed species (carbonates, formates) were also detected during IR adsorption experiments together with perturbations in OH vibrations region.

On admission of successive CO doses on Pd/YSZ wafer at room temperature, IR bands recorded at 2094, 1981, 1942 and 1879 cm^{-1} increase until surface saturation (spectrum (a)). Note that attributions can be difficult in the light of the outcome results of the literature, but the band at 2094 cm^{-1} is tentatively assigned to monocarbonyls species bound to Pd metal particles (linear Pd^0–CO), while bands at 1981 and 1942 cm^{-1} are attributed to compressed and isolated bridged carbonyls respectively where a single CO molecule is adsorbed on two Pd^0 sites (Pd_2–CO). Compressed term means that two bridged species are quite close to interact together; in other words each Pd adsorption center is bound to two CO bridging molecules. Such a configuration would be preferentially found on (111) faces of larger Pd metal particles due to their pillbox morphology.[19] The shoulder at 1879 cm^{-1} is associated with triply bridging carbonyls species (Pd_3–CO).[18]

Table 1. Assignment of IR bands (νCO) corresponding to CO adsorbed species on Pd^0 sites observed in Figure 4 [18,19]

Conditions	Pd^0-CO (cm^{-1})	$(Pd^0)_2$-CO[a] (cm^{-1})	$(Pd^0)_2$-CO[b] (cm^{-1})	$(Pd^0)_3$-CO (cm^{-1})
FTIR-$T_{amb.}$	2094	1981	1942	1879
DRIFTS-$T_{amb.}$	2094	1973	1915	n.d.
DRIFTS-425°C	2070	1940	n.d.	n.d.
POM-425°C	2056	1915	n.d.	n.d.

[a] Compressed carbonyls. [b] Isolated bridged carbonyls.

It has been observed that DRIFTS spectra, realized at ambient temperature (spectrum (b)), were quite similar to FTIR spectra whereas an increase at 425°C (spectrum (c)) resulted in a red shift of vibrations modes towards lower wavenumbers (2070 and 1940 cm^{-1} for Pd^0–CO and Pd_2–CO respectively). Comparing this latter with spectra recorded during POM reaction at 425°C (spectra (d)), a light shift of the bands of CO adsorbed species has also been denoted, resulting in IR bands at 2056 and 1915 cm^{-1} for linear and bridged adsorbed carbonyls. This shifting could be linked to a difference of surface coverage during the catalytic oxidation reaction, together with a temperature effect. Additionally the reducing environment of the POM reaction can also contribute to enhance the red shift of the $2\pi^*$ back-donation by strengthening the metallic palladium state. Note that the amount of linear Pd^0–CO adsorbed species, less stable than bridged one, is smaller at 425°C.

Observation of intermediate species

In order to highlight the formation of intermediate species during POM reaction, further analysis of DRIFTS spectra was performed in which the spectrum obtained at 35.0 min of reaction over Pd/YSZ from Figure 2A, is subtracted to the following spectra to highlight the adsorbed species. Results reported in Figure 5 show that distinct IR bands appear simultaneously from 39.6 min at 1355, 1382, 1576 and 2879 cm^{-1}. According to previous numerous studies [20-23], these wavenumbers are characteristic of

Accepted Manuscript

This article is protected by copyright. All rights reserved.

10.1002/cssc.201601165

stretching and deforming modes of the formate species ($HCOO^-$) adsorbed on the YSZ oxide, as reported in Table 2. Note that maximum of IR formate bands intensity was obtained as of 47.6 min.

The formation of formate species adsorbed on YSZ surface can be explained by two hypotheses. They can be (i) formed from carbon monoxide or (ii) an intermediate species driving the CO yield. Characteristic $HCOO^-$ bands were not observed previous to 40 min of reaction which means that they could react very quickly to produce the products mentioned upstream.

Table 2. Assignment of the adsorbed formate vibration bands.

Catalysts	νCH (cm^{-1})	ν_{as}OCO[a] (cm^{-1})	ν_sOCO[b] (cm^{-1})	δCH (cm^{-1})	ν_{as}OCO + δCH overtone (cm^{-1})
Pd/YSZ	2879	1576	1355	1382	n.d.
YSZ	2880	1574	1357	1383	2968

[a] Suffix "as" for asymmetric. [b] Suffix "s" for symmetric

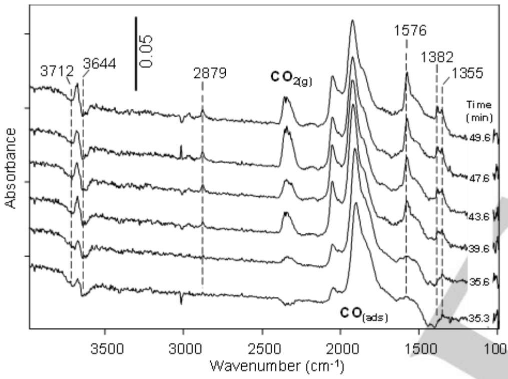

Figure 5. Identified formate species ($HCOO^-$) adsorbed on Pd/YSZ surface during POM reaction at 425°C.

Even if the first option cannot be totally excluded, the second one was preferentially admitted for a number of reasons (see discussion). On the one hand, when the temperature of reaction increases, IR bands of formate species disappear while CO production increases in gas phase. It indicates that carbon monoxide could be formed after $HCOO^-$ decomposition. Supplementary POM experiment was performed over YSZ oxide, without Pd deposition, at 425°C using isotopic exchange-DRIFTS coupling. Figure 6A shows IR spectra recorded during this reaction and MS signals are reported in Figure 7. Surprisingly, IR bands assigned to formate adsorbed species were clearly observed at 1357, 1383, 1575 and 2880 cm^{-1} with a relatively high intensity and increasing with time on stream. A new vibration frequency was also detected at 2968 cm^{-1} which is attributed to a combination between ν_{as}OCO and δCH modes (Table 2).

Concurrently, MS profiles (Figure 7) shows a poor methane conversion with relatively no $^{18}O_2$ consumption. It means that gaseous oxygen is not consumed in YSZ system at 425°C even in presence of CH_4. This observation proves that carbon monoxide is not responsible for the formate species formation on YSZ surface which invalidates the first hypothesis mentioned before. Nevertheless, when the temperature was raised at 700°C, results show the exclusive formation of CO_2 in gas phase, without syngas production (Figure 7). IR spectra recorded at the same time and represented in Figure 6B also confirm the CO_2 production (2260-2400 cm^{-1}) with a simultaneous consumption of formate adsorbed species (negative IR bands). This result is in accordance with previous study [24] suggesting a decomposition of formate species to produce CO_2 molecule. Finally, in the region of hydroxyl groups, negative IR bands around 3671-3675 cm^{-1} can be attributed to water desorption.

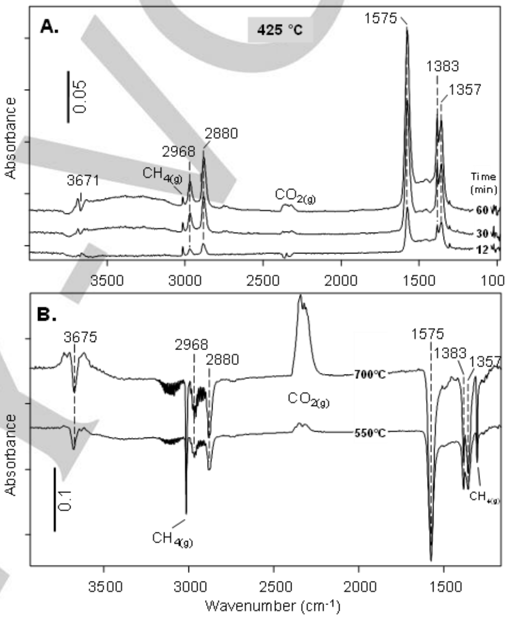

Figure 6. Identification of formate adsorbed species on YSZ surface during POM reaction **A.** at 425°C and **B.** between 425-700 °C.

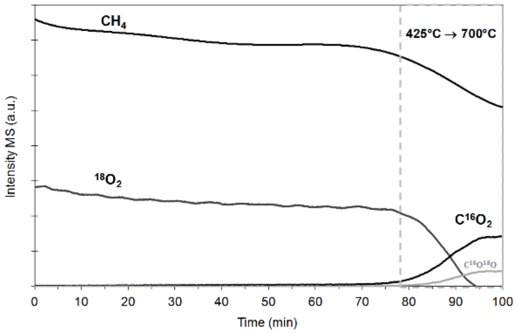

Figure 7. MS profiles of gas phase from POM reaction over YSZ support.

A last important point to stress is the formation of intermediate $HCOO^-$ species from lattice oxygen atoms of YSZ material involving *MvK* mechanism during POM reaction. Indeed, no isotopic shifting of stretching νOCO modes was observed while labeled isotope $^{18}O_2$ was introduced in gas phase at the beginning of the reaction. Thus, the decomposition of $HC^{16}O^{16}O^-$ intermediate species can explain the formation of unlabeled

Accepted Manuscript

This article is protected by copyright. All rights reserved.

products $C^{16}O_2$ and $C^{16}O$ during POM reaction on Pd/YSZ and dual LM-Pd/YSZ bed catalysts.

Discussion of reaction mechanism

As mentioned previously, the role of formate species is an essential step in the mechanism of synthesis gas production during the partial oxidation of methane. Several mechanisms are developed to highlight the formation mechanism of formate species. It is reported that both acidic hydroxyls and O^{2-} ions could play an important role in the generation of these species. Carbon monoxide can hypothetically reacts with hydroxyls to form formate species, leading to the consumption of an OH group, revealing that OH groups surface could also behave as active sites for CO transformations. For instance, by means of *in-situ* transmission FTIR experiments, Lefferts *et al*. reports that hydroxyl groups on the ZrO_2 support are involved in the formate yield by reaction with CO. In the presence of metallic supported catalyst (Pt/ZrO_2) formate decomposition can thereafter lead to H_2 and CO_2 production.[25] On ceria-based catalysts, Shido and Iwasawa[26] used infrared spectroscopy to conclude that bidentate formate species are produced by the reaction of CO with terminal hydroxyl groups of the ceria surface and that these species can be decomposed into H_2 and carbonate species. More recently, Li *et al*.[27] have invoked a redox process to explain the mechanism of formation of formate species. These authors conclude that CO adsorbs on metal sites and reacts with the neighbouring framework oxygens. The reduced oxide can furthermore be oxidized by CO_2. Even if this process cannot be totally excluded, since CO adsorption has revealed the presence of metallic Pd sites (Figure 4), formate compounds are rather assumed to be responsible of the syngas production as intermediate species of CH_4 activation. Whatever the active sites considered (*i.e*. PdO or $O^{-}_{(s)}$), surface formate formation involves dissociation to adsorbed methyl or methylene radicals as a result of the removal of hydrogen atoms from the methane. CO, CO_2, H_2 and H_2O being the major decomposition products of formate intermediate species, in agreement with the results presented here.

The nature of active sites of Pd catalysts for methane oxidation has been a matter of debate for a long time. It has been thought that the active form of palladium is an oxidized state, but the precise nature of the active sites is still controversy since it remains conflicting evidence on the activity of different oxidation states of Pd for methane oxidation. Nevertheless, it has been reported that methane is activated on a site pair consisting of an oxygen atom and an oxygen vacancy site on the PdO surface, suggesting a redox mechanism[28,29] where surface oxygen on the palladium crystallites is much higher active for methane oxidation than bulk oxide of palladium due to the higher ability of the oxygen sorption processes.[30] Methane interacts with oxygen on the PdO surface which is rapidly restored by diffusion of bulk oxygen to the surface, which perfectly matches with the dramatic enhancement of methane oxidation observed on the LM-Pd/YSZ dual bed system (Figure 1). To the opposite, methane oxidation over the metallic Pd surface is controlled by competitive adsorption of methane and oxygen.

Activation of the methane molecule is often proposed to be the rate-limiting step of the reaction over both the Pd and the PdO states. However, at low to moderate temperatures (T<450°C) the recombination of surface hydroxyl and water desorption from the catalyst can likely control reactivity of methane oxidation over PdO, making the water desorption from the surface the rate-limiting step for methane oxidation.[31] The poisoning effect of water was proposed to be due to the formation of palladium (II) hydroxide where the breaking of the OH bond in the hydroxide is the determining-step.[32] The influence of water on the catalyst activity is also affected by the type of host materials where high oxygen mobility supports show potential to moderate inhibition by water, accelerating hydroxyl desorption.[33] In addition, the oxygen mobility of the support can strongly affect the oxidation/reduction behavior of palladium particles together with the reversibility of water poisoning.

The initial step in methane activation on noble metal involves assisted hydrogen abstraction.[34] The subsequent interaction of the methyl or methylene radicals with the adsorbed oxygen has been proposed to lead to either direct combustion to carbon dioxide and water or the formation of chemisorbed formaldehyde via methoxide, methyl peroxide, or methylene oxide intermediates.[30,35] Consequently, the first step of the POM experiments presented herein (Figure 1, Figure 2B) is in accordance with the literature data above presented. Methane conversion is enhanced over palladium containing catalyst by assisting the complete CH_4 combustion together with CO_2 yield, leading to oxygen consumption. Thereafter, the remaining methane is converted to synthesis gas by direct or indirect POM.

Over non-noble catalysts, the first step for methane oxidation is also the dissociative adsorption of methane leading to Metal-CH_3 bond together with a hydroxyl group formation. This first step can be catalysed by Lewis acid sites and adjacent lattice oxygen [36] but Steghuis *et al.* [37] agrees that methane is rather homolytically dissociated over coordinatively unsaturated oxygen sites ($O^{-}_{(s)}$) of yttria-zirconia materials to form methoxy and subsequently formate adsorbed species. Zhu *et al.*[24] also suggest that formate species are formed by methane reaction with lattice oxygen atoms of YSZ catalyst, as illustrated in Figure 6. The rate-determining step is suggested to be likely the splitting of a Metal-CH_3 bond. Thereafter, C−H bond in the methoxy is dissociated to form a second OH group and the remaining OCH_2 forms a dioxymethylene which is considered as formaldehyde precursor.[38,39] Formaldehyde is never observed due to rapid conversion to formate. In a recent DFT study, Cooper *et al.* reported an energetically favourable methane C–H bond cleavage over YSZ in the presence of oxygen.[40] In this mechanism, oxygen is activated on the YSZ surface as a superoxide like species. On the neighbouring surface oxygen ions H abstraction occurs and the C–H bond of the methane undergoes homolytic breaking, forming hydroxyl group with an overall -1 charge, the additional electron density being transferred to the superoxide species.

Finally, the methane C–H bond activation therefore implies the activation of O_2 and the formation of the methyl radical would be the first step of the formation of formaldehyde or formate species. This mechanism occurs at 425°C with appearance of the vibration bands of the formate species on the spectra collected over single YSZ (Figure 6). No formation of gaseous products was evidenced

Accepted Manuscript

This article is protected by copyright. All rights reserved.

WILEY-VCH
Accepted Manuscript

at this temperature because of the stability of the formate species on the YSZ surface in agreement with the work of Zhu *et al.* who demonstrated in the same domain of temperature that the rate-determining step of POM over YSZ (with 12mol%Y_2O_3) was not activation of methane but decomposition of the formate.[24] In single YSZ, dissociation of superoxide species is limited and production of combustion product is not observed. An increase of the temperature is needed to decompose the formate species generating CO_2 and H_2O (Figure 7). In the dual bed system we demonstrated in a previous work[10,11] that the first $LaMnO_3$ bed acted as a generator of highly reactive intermediate singlet ($^1\Delta_g$) molecular oxygen making its dissociative activation possible at lower temperature over the YSZ surface. We observed here that it increases the rate of decomposition of the formate species since the generation combustion CO_2 and H_2O products was observed for LM-YSZ in larger amount than for single LM catalyst. Accordingly, the dramatic enhancement of synthesis gas production in the $LaMnO_3$-Pd/YSZ dual bed system is tentatively attributed to higher activation of O_2 molecule on YSZ surface vacancies, that enables a rapid recovery of surface PdO species required for the decomposition of adsorbed formate species to CO and CO_2 molecules in gas phase. In absence of oxygen, oxidation of formate species into CO_2 and H_2O is inhibited and selectivity to synthesis gas generation is increased due to the formates dehydration into CO and H_2O and formates dehydrogenation into CO_2 and H_2.[41,42] However if the formation of synthesis gas was observed on pure YSZ at very high temperature by Zhu *et al.*,[43] the necessity of Pd particles is essential at moderate temperatures.

Conclusions

The objective of this work was to investigate the mechanism of low-temperature methane oxidation over a highly active catalyst. An innovative dual-bed system, $LaMnO_3$-Pd/YSZ was studied showing a remarkable improvement of the catalytic oxidation activity in both methane combustion and synthesis gas production. Arrangement of a DRIFTS cell in a closed recycling system of isotopic exchange set-up allows the observation of adsorbed intermediates species on catalytic surface during the partial oxidation of methane (POM) reaction at 425°C and enables to highlight the synthesis gas production mechanism. While the use of labeled oxygen ($^{18}O_2$) reactant, unlabeled oxidation products ($C^{16}O_2$, $H_2{}^{16}O$, $C^{16}O$) were mainly detected by mass spectrometry in gas phase involving the participation of lattice oxygen atoms from YSZ material in the reaction via a so-called *Mars van Krevelen* mechanism. Similar behavior was found for Pd/YSZ catalysts which was used to perform ^{18}O labeling-DRIFTS coupling experiments. At this temperature, CO molecule is adsorbed on Pd sites revealing infrared bands in the 1675-2095 cm^{-1} spectral range assigned to linear and bridged carbonyl adsorbed species. The attribution of these vibration frequencies was confirmed with isotopic shifting observed in the case of the reaction over a pre-exchanged catalyst. IR analysis also reveals the formation of formate species ($HCOO^-$) adsorbed on YSZ surface during POM reaction. According to previous study and results obtained with bare YSZ material, we supposed that this former plays a role of intermediate species in POM reaction. In this case, formate species results from methane activation and lattice oxygen atoms of YSZ.

Experimental Section

Materials

The preparation and characterization of the materials used in this study have already been described elsewhere [44]. The citrate route was selected to synthesize $LaMnO_3$ perovskite in which equimolar amounts of two metal nitrates precursors, $La(NO_3)_3{\cdot}6H_2O$ (Sigma Aldrich, >99.0%) and $Mn(NO_3)_2{\cdot}4H_2O$ (Alfa Aesar, 98%), were mixed in 25 cm^3 distilled water. After addition of anhydrous citric acid (Alfa Aesar, >99.5%), the solution was heated at 90°C for 2h to evaporate excess H_2O under magnetic stirring (600 rpm), then dried at 110°C overnight. After milling, the sample was submitted to a static thermal treatment in an oven up to 200°C (ramp rate 1°C min^{-1}) to eliminate the citric acid. The resulting $LaMnO_3$ catalyst was finally calcined at 750°C for 2h with a ramp rate of 5°C min^{-1} by using a quartz tubular reactor under air flow (50 cm^3 min^{-1}) and exhibits a specific surface area of 20 m^2 g^{-1}. In Figure 8, powder X-ray diffraction (XRD) pattern shows well-crystallized samples without any presence of amorphous regions corresponding to the expected $LaMnO_3$ phase. The mean crystallite size of bulk perovskite determined from line-broadening of the most intense reflections at 32.6° using the Scherrer equation is ≈14.8 nm.

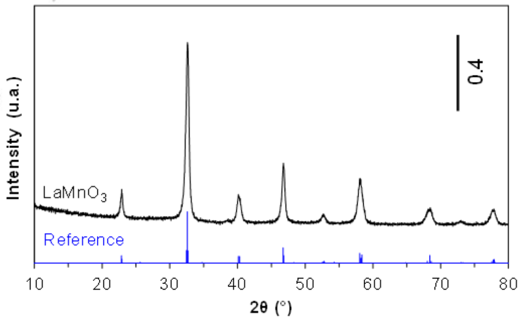

Figure 8. XRD pattern of $LaMnO_3$ material. Reference corresponds to the expected $LaMnO_3$ phase (ISCD file 98-008-2226).

YSZ (8_{mol}% Y_2O_3-stabilized ZrO_2) oxide was provided by TOSOH. This commercial material was calcined at 750°C (5°C min^{-1}) under air flow (50 cm^3 min^{-1}) for 2h before use. YSZ exhibits a specific surface area of 13 m^2 g^{-1} and a cubic fluorite structure [1]. The mean crystallite size of the YSZ oxide is ≈18.2 nm. Finally YSZ-supported Pd catalysts (Pd/YSZ) were prepared by wet impregnation of the appropriate amount of nitrate precursor $Pd(NO_2)_2(NH_3)_2$ (Alfa Aesar, 8.91_{mass}% Pd) to obtain 0.2 $_{wt}$% Pd. The excess water was evaporated by using sand bath at 60°C. The resulting solid was dried at 120°C overnight and calcined at 700°C during 4h under air flow (60 cm^3 min^{-1}). Amount of 0.297 $_{wt}$% Pd was determined by inductively coupled plasma optical emission spectroscopy (ICP-OES).

^{18}O labeling-DRIFTS coupling set up

This article is protected by copyright. All rights reserved.

The ^{18}O labeling-DRIFTS coupling set up is depicted in Figure 9 and consisted of three main parts: (i) a DRIFTS cell connected to (ii) a closed recycling system and (iii) the analysis section.

The DRIFTS cell (Praying Mantis™ from Harrick Scientific Products) consists of a high temperature reaction chamber placed in a highly efficient diffuse collection system (6 mirrors) that minimizes the detection of the specular component. The reaction chamber was engineered to perform studies under controlled temperatures (up to 910°C) and pressures (from 133 µPa to 133 kPa). Catalyst is deposited under a wire mesh in a ceramic crucible covered with a dome having two KBr windows transparent to IR radiation. The objective of that DRIFTS cell was to observe adsorbates on the catalyst surface. Note that the dead volume (≈3 cm^3), allowing observation of gaseous reactants and products present within the reactor, can also reduce temporal resolution of the IR technique. In our case, the utilization of recycling pump allows to curtail this problem.

Both inlet/oulet ports provided for introducing/evacuating reaction chamber are connected to a closed recycling system already described elsewhere[45]. The whole system (DRIFTS cell + closed system) represents a volume of about 90 cm^3 for a recycling flow of 170 $mL.s^{-1}$.

The analytical instrumentation includes a *mass spectrometer* (Pfeiffer Vacuum, QMS 200 quadrupole, Faraday detector) to monitor the gas-phase composition (mass-to-charge *m/z* signals) and connected to the closed recycle system. A controlled valve was used to limit the operating pressure of the mass spectrometer ionization chamber at 10^{-6} mbar. The DRIFTS cell was placed in a Bruker (Equinox 55) *IR spectrometer* with a MCT (Mercure-Cadmium-Tellure) detector. Spectra were collected in a range of 400 to 4000 cm^{-1}, accumulating 64 scans with a spectral resolution of 4 cm^{-1}. Reference spectra was recorded over a KBr powder sample at ambient temperature under primary vacuum. Spectra were plotted as a function of wavenumber using OPUS® Bruker software after Fourier transform mathematical treatment of single beam interferogram.

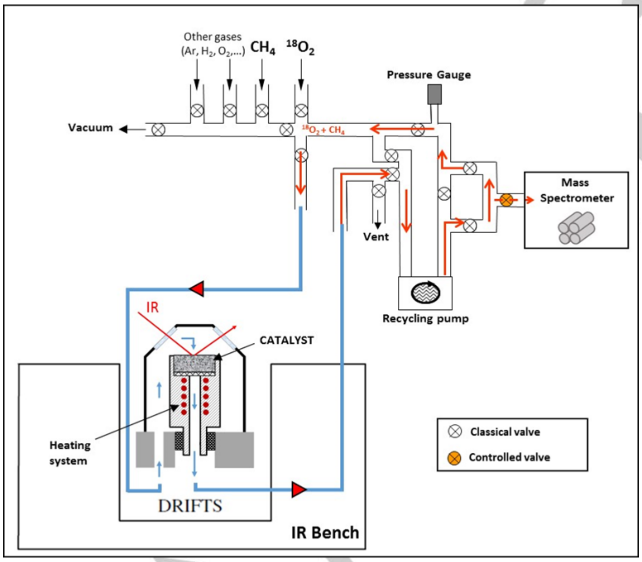

Figure 9. Schematic representation of experimental set up.

Partial oxidation of methane

POM experiments were performed by using the set up described above. Isotherm experiments at 425°C were undertaken on 30 mg $LaMnO_3$ *(+SiC)*, 110 mg Pd/YSZ and 75 mg dual bed material or mechanical mixture placed in the DRIFTS cell reactor.

Before the reaction, sample were additionally subjected to an oxidation activation step at 700 °C for 1h under a $^{16}O_2$ flow before cooling to 425°C at which the system was purged for 30 min using primary vacuum. Then, 105 mbar of a mixture of CH_4:$^{18}O_2$ in a molar ratio 2:1 was introduced in the reactor. The m/z values and corresponding gaseous molecules reported in Table 3 were monitored continuously during the POM reaction as a function of time.

A POM experiments was performed on a pre-exchanged Pd-YSZ catalyst. After same pre-treatment (oxidation and purge), several consecutive $^{18}O_2/^{16}O_2$ exchange reactions were undertaken at 700°C for 20-30 min by introducing each time 50 mbar of $^{18}O_2$ labeled molecule in the reactor. The formation of $^{16}O^{18}O$ and $^{16}O_2$ isotopes in the gas phase indicates that exchange reaction takes place in the catalyst involving YSZ lattice ^{16}O atoms. We estimate after consecutive experiments that around 98% of oxygen atoms are exchanged in the material (*i.e*. 98% of lattice oxygen atoms of YSZ oxide are labeled (^{18}O). After a purge step at 425°C, POM experiments were performed by using protocol described above.

Table 3. Gaseous molecules recorded during POM experiments and corresponding m/z signals.

m/z	Molecule	m/z	Molecule	m/z	Molecule
2	H_2	**28**	N_2, $C^{16}O$,$C^{16}O_2$	**36**	$^{18}O_2$
15	CH_4	**30**	$C^{18}O$, $C^{16}O^{18}O$, $C^{18}O_2$	**44**	$C^{16}O_2$
18	$H_2{}^{16}O$, $^{18}O_2$, $^{16}O^{18}O$	**32**	$^{16}O_2$	**46**	$C^{16}O^{18}O$
20	$H_2{}^{18}O$	**34**	$^{16}O^{18}O$	**48**	$C^{18}O_2$

FTIR CO-adsorption

A self-supporting wafer (ca. 15 mg cm^{-2}) was prepared by pressing Pd/YSZ powder at 100 bar. Then, the sample was introduced in the IR cell connected to a vacuum and adsorption system. Prior to the adsorption measurement, the catalyst was pre-treated at 450°C (ramp rate 10°C min^{-1}) under H_2 flow (30 cm^3 min^{-1}) for 1h. Then, the system was purged at the same temperature for 45 min by using secondary vacuum (10^{-3} Pa). The wafer was cooled at room temperature under vacuum in the T-shaped IR cell provided with two KBr windows transparent to IR beam.

Successive doses of carbon monoxide (Pressure = 0.1 to 100 mbar in a volume of 0.9 cm^3) were introduced at ambient temperature on the wafer until surface saturation. A spectrum was collected after each addition of CO in the IR cell, in a range of 400 to 4000 cm^{-1}, accumulating 64 scans with a spectral resolution of 4 cm^{-1}. Spectra (a) in Figure 4 was recorded after introduction of around 1.8×10^{-5} mol of CO. Nicolet 6700 apparatus with a MCT detector was used to realize FTIR CO-adsorption experiments. Absorbance spectra were plotted as a function of wavenumber using OMNIC® software.

Keywords: Partial oxidation • Methane • Isotopic exchange • DRIFTS • Yttrium-stabilized zirconia

[1] R. Horn, R. Schlögl, *Catal. Lett.* **2015**, *145*, 23-39.

[2] P. Gélin, M. Primet, *Appl. Catal. B: Environ*. **2002**, *39*, 1-37.

Accepted Manuscript

This article is protected by copyright. All rights reserved.

[3] P. Castellazzi, G. Groppi, P. Forzatti, A. Baylet, P. Marécot, D. Duprez, *Catal Today* **2010**, *155*, 18-26.
[4] S. Royer, D. Duprez, F. Can, X. Courtois, C. Batiot-Dupeyrat, S. Laassiri, H. Alamdari, *Chem. Rev*. **2014**, *114*, 10292-10368.
[5] O. Boucher, P. Friedlingstein, B. Collins, K. P Shine, *Environ. Res. Lett*. **2009**, 4, 044007.
[6] D. A. Lashof, D. R. Ahuja, *Nature* **1990**, *344*, 529-531.
[7] A. T. Ashcroft, A. K. Cheetham, J. S. Foord, M. L. H. Green, C. P. Grey, A. J. Murrell, P. D. F. Vernon, *Nature* **1990**, *344*, 319-321.
[8] C. Hammond, S. Conrad, I. Hermans, *ChemSusChem* **2012**, *5*, 1668-1686.
[9] C. Berger-Karin, M. Sebek, M.-M. Pohl, U. Bentrup, V. A. Kondratenko, N. Steinfeldt, E. V. Kondratenko, *ChemCatChem* **2012**, *4*, 1368-1375.
[10] M. Richard, F. Can, D. Duprez, S. Gil, A. Giroir-Fendler, N. Bion, *Angew. Chemie, Int. Ed*. **2014**, *53*, 11342-11345.
[11] M. Richard, F. Can, D. Duprez, S. Gil, A. Giroir-Fendler, N. Bion, *ChemCatChem* **2016**, *8*, 1921-1928
[12] J. J. Zhu, M. S. M. M. Rahuman, J. G. van Ommen, L. Lefferts, *J. Catal.* **2005**, *233*, 434-441.
[13] R.J. Farrauto, M.C. Hobson, T. Kennelly, E.M. Waterman, *Appl. Catal. A: Gen*. **1992**, *81*, 227-237.
[14] N. Takahashi, M. Sate, M. Nagumo and A. Mijin, *Zeolites* **1986**, *6*, 420-422.
[15] W.R. Schwartz, L.D. Pfefferle, *J. Phys. Chem. C* **2012**, *116*, 8571-8578.
[16] K.I. Hadjiivanov and G.N. Vayssilov, *Adv. Catal*. **2002**, *47*, 307-511.
[17] K. Wolter, O. Seiferth, J. Libuda, H. Kuhlenbeck, M. Bäumer, H.J. Freund, *Surf. Sc.* **1998**, *402-404*, 428-432.
[18] M. A. Vannice, S-Y. Wang, S. H. Moon, *J. Catal*. **1981**, *71*, 152-166.
[19] W. Daniell, H. Landes, N.E. Fouad, H. Knözinger, *J. Mol. Catal. A: Chemical* **2002**, *178*, 211-218.
[20] E. Finocchio, M. Daturi, C. Binet, J.C. Lavalley, G. Blanchard, *Catal. Today*, **1999**, *52*, 53-63.
[21] G. Jacobs, L. Williams, U. Graham, G.A. Thomas, D.E. Sparks, B.H. Davis, *Appl. Catal. A: Gen.* **2003**, *252*, 107-118.
[22] G. Busca, J. Lamotte, J.C. Lavalley, V. Lorenzelli, *J. Am. Chem. Soc*., **1987**, *109*, 5197-5202.
[23] E.-M. Köck, M. Kogler, T. Bielz, B. Klötzer, S. Penner, *J. Phys. Chem. C* **2013**, *117*, 17666-17673.
[24] J. Zhu, J. G. van Ommen, L. Lefferts, *J. Catal*. **2004**, *225*, 388-397.
[25] P.O. Graf, D.J.M. de Vlieger, B.L. Mojet, L. Lefferts, *J. Catal*. **2009**, *262*, 181-187.
[26] T. Shido, Y. Iwasawa, *J. Catal*. **1993**, *141*, 71-81.
[27] Y. Li, Q. Fu, M. Flytzani-Stephanopoulos, *Appl. Catal., B*. **2000**, *27*, 179-191.
[28] K. Fujimoto, F. H. Ribeiro, M. Avalos-Borja, E. Iglesia, *J. Catal*. **1998**, *179*, 431-442.
[29] J. Au-Yeung, K. Chen, A.T. Bell, E. Iglesia, *J. Catal*. **1999**, *188*, 132-139.
[30] C.F. Cullis, B.M. Willat, *J. Catal*. **1983**, *83*, 267-285.
[31] R. Burch, F.J. Urbano, *Appl. Catal. A: Gen*. **1995**, *124(1)*, 121-138.
[32] R. Burch, D.J. Crittle, M.J. Hayes, *Catal. Today* **1999**, *47*, 229-234.
[33] D. Ciuparu, E. Perkins, L. Pfefferle, *Appl. Catal. A: Gen*. **2004**, *263*, 145-153.
[34] K.D. Campbell, E. Morales, J.H. Lunsford, *J. Am. Chem. Soc*. **1987**, *109(25)*, 7900-7901.
[35] G.B. Hoflund, Z.H. Li, W.S. Epling, T. Göbel, P. Schneider, H. Hahn, *React. Kinet. Catal. Lett*. **2000**, *70*, 97-103.
[36] V.D. Sokolovskii, S.M. Aliev, O.V. Buyevskaya, A.A. Davydov, *Catal. Today* **1989**, *4*, 293-300.
[37] A.G. Steghuis, J.G. van Ommen, J.A. Lercher, *Catal. Today*, **1998**, *46*, 91-97.
[38] C.F. Cullis, B.M. Willatt, *J. Catal*., **1983**, *83*, 267-285.
[39] Z. Li, G.B. Hoflund, *J. Nat. Gas Chem.* **2003**, *12*, 153-160.
[40] C. S. Cooper, R. J. Oldman, C. R. A. Catlow, *Chem Commun*. **2015**, *51*, 5856−5859.
[41] D.C. Grenoble, M.M Estadt, D.F. Ollis, *J. Catal*. **1981**, *67*, 90-102.
[42] D. Bianchi, T. Chafik, M. Khalfallah, S. J. Teichner,*Appl. Catal. A: Gen.* **1993**, *105*, 223-249.
[43] J. Zhu, J. G. van Ommen, L. Lefferts, Catal. Today **2006**, *117*, 163–167.
[44] A. Giroir-Fendler, M. Alves-Fortunato, M. Richard, C. Wang, J. A. Díaz, S. Gil, C. Zhang, F. Can, N. Bion, Y. Guo, *Appl. Catal. B: Environ* **2016**, *180*, 29-37.
[45] D. Martin, D. Duprez, *J. Phys. Chem*. **1996**, *100*, 9429–9438.

WILEY-VCH

Accepted Manuscript

This article is protected by copyright. All rights reserved.

FULL PAPER

The dual $LaMnO_3$-0.2%$_{wt}$Pd/YSZ catalytic system is highly active for CH_4 partial oxidation at moderate temperatures. The role of $LaMnO_3$ is to generate active singlet oxygen species in order to improve the oxygen activation step on the YSZ surface. The rate of oxidation of methane which followed a *MvK* mechanism is then drastically increased and intermediate formate species can subsequently be decomposed into CO and H_2.

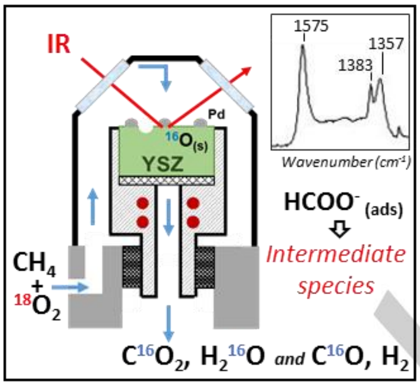

*Melissandre Richard, Daniel Duprez, Nicolas Bion, Fabien can**

Page No. – Page No.

Investigation of methane oxidation reactions over Lanthanum Manganites-Pd/YSZ dual bed by ^{18}O labeling-DRIFTS coupling

WILEY-VCH

Accepted Manuscript

This article is protected by copyright. All rights reserved.